thermoscientific

TECHNICAL NOTE 30396

10^{13} AMPLIFIER TECHNOLOGY

Dynamic time correction for high precision isotope ratio measurements

Thermo Scientific Neptune Plus MC-ICP-MS with 10^{13} Ω amplifier technology

Authors

Grant Craig,[1] Zhifang Hu,[2] Anyu Zhang,[2] Nicholas S. Lloyd,[1] Claudia Bouman[1] and Johannes Schwieters[1]

[1]Thermo Fisher Scientific, Bremen, Germany

[2]Thermo Fisher Scientific, China

Keywords

Neptune Plus MC-ICP-MS, Laser Ablation, 10^{13} Ω Amplifier, Isotope Ratio, Tau Correction, Transient Signal Analysis

Abstract

To demonstrate the application of dynamic, response time-based, correction to high precision isotope ratio measurements on the Thermo Scientific™ Neptune Plus™ MC-ICP-MS, using 10^{13} Ω amplifier technology.

Introduction

With multicollector mass spectrometers, low intensity ion beams are typically collected on ion counters rather than with Faraday cup collectors, as the precision of Faraday cup measurements would be limited by the electrical noise of the standard 10^{11} Ω amplifiers.[1] A recent development in the evolution of multicollector inductively coupled plasma mass spectrometry (MC-ICP-MS) has been the introduction of Faraday cup amplifiers incorporating 10^{13} Ω resistors.[2] Compared to the standard 10^{11} Ω amplifier, the signal-to-noise ratio of the 10^{13} Ω amplifier is improved by 4 to 5 fold; which should correspond to a similar improvement in isotope ratio precision for analyses of small ion beams.[3] Consequently many of the applications that previously required ion counters can now be measured with 10^{13} Ω amplifiers.

One of the primary advantages of MC-ICP-MS is the simultaneous detection of multiple isotopes. Static multicollection with an array detector ensures no ions are lost, maximizing the duty cycle. However, while it is true to say the ions are collected simultaneously, it is not true to state they registered simultaneously.

ThermoFisher SCIENTIFIC

Relative to an ion counting detector, Faraday cup detectors experience a time offset and tau decay, due to the response on the associated amplifier. These differences in the signal response and decay of Faraday cup detectors have been reported to bias isotope ratio results.[5] The signal response and decay of Faraday cups coupled to amplifiers with 10^{13} Ω resistors are significantly slower than those using standard 10^{11} Ω resistors. Klaver et al[4] noted, that the successful application of 10^{13} Ω amplifiers to Pb isotope ratio analysis by thermal ionization mass spectrometry (TIMS) requires a stable ion beam in order to control for the slow response and decay times. However, 10^{13} Ω amplifiers have been applied with laser ablation (LA-) MC-ICP-MS, a technique for which stable ion beam intensities are rarely achieved.[6] To compensate for the slow response and decay times of the 10^{13} Ω amplifiers, Kimura *et al*[2] applied a mathematical correction. This was described first for LA-ICP-MS with 10^{11} – 10^{12} Ω amplifers.[7-9] The correction takes advantage of a linear relationship between the isotope ratio and the rate of change of the signal intensity, with the slope of the resulting regression line used to produce a corrector factor for the measured isotope data.

Therefore, in order to achieve the best possible accuracy and precision using Faraday detector systems with 10^{13} Ω amplifiers, correction for the slow response and decay times may be required. By determining the tau decay constant for each 10^{13} Ω amplifier, a dynamic time correction can be applied to the measured signal intensity rather than the measured ratio. In this way, isotope ratio drift due to the response time of each amplifier may be corrected independently of other changes in isotope ratio, such as sample heterogeneity.

Method

The laser ablation system used was a Teledyne Photon Machines Analyte G2™ excimer laser with 193 nm wavelength. The laser was equipped with a HelEx™ II two-volume ablation cell. Operating conditions are given in Table 1 and the cup configurations used outlined in Table 2. The system was tuned prior to analysis by line ablation of NIST™ SRM® 612. Pb isotope ratio analysis ($^{208}Pb/^{206}Pb$ and $^{207}Pb/^{206}Pb$) was performed on four MPI-DING glasses. In each of the four MPI-DING glasses (T1-G, ATHO-G, GOR132-G and StHs/680-G) 10 individual spots were ablated. Spot ablations of NIST SRM 612 under identical ablation conditions were used as an external reference. The spot ablations were expected to generate responses with drifting beam intensities, requiring tau correction to achieve the best precision possible.

Table 1. Experimental configuration of the laser ablation and MC-ICP-MS systems. For preparation of the tau correction (tau constants, gain constants) an Teledyne Cetac Technologies Aridus™ II (Ar – 3.98 L min^{-1}, N_2 – 6 mL min^{-1}) was used, aspirating a 2.5 ppb Certipur™ Neodymium solution.

Analyte G2™ Laser Ablation		Neptune Plus MC-ICP-MS	
Parameter	**Value**	**Parameter**	**Value**
Fluence (J cm^{-2})	3	Cool Gas (L min^{-1})	16
Repetition Rate (Hz)	8	Auxiliary Gas (L min^{-1})	0.85
Spot Shape	Circle	Sample Gas (L min^{-1})	0.75
Spot Size (µm)	40	Power (W)	1200
Duration (s)	30	Skimmer Cone	X
He Outer Cell (L min^{-1})	0.70	Sample Cone	Jet
He Cup Flow (L min^{-1})	0.45	Resolution	Low
N_2 Addition (mL min^{-1})	11.0		

Table 2. Cup configurations on Neptune Plus MC-ICP-MS. Nd cup configuration was used to determine gain calibration and tau constant factors for 10^{13} Ω amplifiers. Pb cup configuration was used for analysis.

Configuration		L4	L3	L2	L1	C	H1	H2	H3	H4
Nd	Mass	^{140}Ce	^{142}Nd	^{143}Nd	^{144}Nd	^{145}Nd	^{146}Nd	^{147}Sm	^{148}Nd	^{150}Nd
	Amplifier	10^{11} Ω	10^{11} Ω	10^{11} Ω	10^{11} Ω	10^{13} Ω	10^{11} Ω	10^{11} Ω	10^{13} Ω	10^{13} Ω
Pb	Mass		^{202}Hg	^{203}Tl	^{204}Pb	^{205}Tl	^{206}Pb	^{207}Pb	^{208}Pb	
	Amplifier		10^{11} Ω	10^{11} Ω	10^{11} Ω	10^{11} Ω	10^{13} Ω	10^{13} Ω	10^{11} Ω	

Preparation of 10^{13} Ω amplifiers

Gain calibration of 10^{13} Ω amplifiers

Prior to analysis the gain factors for each 10^{13} Ω amplifiers were calibrated. A constant signal was supplied by aspiration of a Certipur™ Neodymium solution (Merck KGaA., Germany), diluted to a concentration of 2.5 ppb in 3% w/w nitric acid, using a Teledyne Cetac Technologies™ Aridus™ II desolvating nebulizer system.

Two nearly identical cup configurations were created; in the first every Nd isotope was assigned to a 10^{11} Ω amplifier. In the second Nd cup configuration the three 10^{13} Ω amplifiers in the Neptune Plus MC-ICP-MS were assigned to ^{145}Nd, ^{148}Nd and ^{150}Nd. (Table 2). In alternate runs the three ratios ^{145}Nd/^{144}Nd, ^{148}Nd/^{144}Nd and ^{150}Nd/^{144}Nd were determined with either 10^{13} or 10^{11} Ω amplifiers assigned to the numerator isotope. Using the following formula gain calibration factors were determined for each 10^{13} Ω amplifier.

$$Gain\,(new)_i = \frac{(10^{11})^x\, Nd/^{144}Nd_{i-1} + (10^{11})^x\, Nd/^{144}Nd_{i+1}}{2 \times (10^{13})^x\, Nd/^{144}Nd_i \times Gain\,(old)}$$

For convenience the previous gain values were set to 0.01. The gain correction factors of the three 10^{13} Ω amplifiers were determined as 0.010151, 0.010158 and 0.010155. The uncertainty on each calibration factor was ≈50 ppm 1RSD (n = 3). The gains are typically stable over periods of several months, and gain determination is recommended on a weekly basis only.

Determination of tau constant for 10^{13} Ω amplifiers

The tau decay constants of the three 10^{13} Ω amplifiers were determined following gain calibration, using the same Nd cup configuration (Table 2). A constant signal was supplied by aspiration of the same 2.5 ppb Nd solution. Ten artificial tau responses and decays were induced in the steady beam intensities by controlled opening and closing of the analyzer gate valve. To best characterize the shape of the tau response a short integration time (66 ms) was selected.

In order to determine the tau constant for each amplifier, an exponential offset function was fitted to each of the tau decay curves generated.

$$I_m = I_o + \Delta I e^{\left\{\frac{-(t_m - t_o)}{t}\right\}}$$

In the exponential offset function I_m is the measured signal intensity at time t_m and I_0 the measured intensity at the start of the decay curve, t_0. Curve fitting was performed within the software platform Igor Pro™ v6.37 (WaveMetrics, Inc., USA) (Figure 1). The tau (τ) constants for each of the three 10^{13} Ω amplifiers were 0.6524 ± 0.0006, 0.6497 ± 0.0008 and 0.6406 ± 0.0010 (n=10). Tau values should be determined after installation or re-installation, but are expected to remain stable over extended periods.

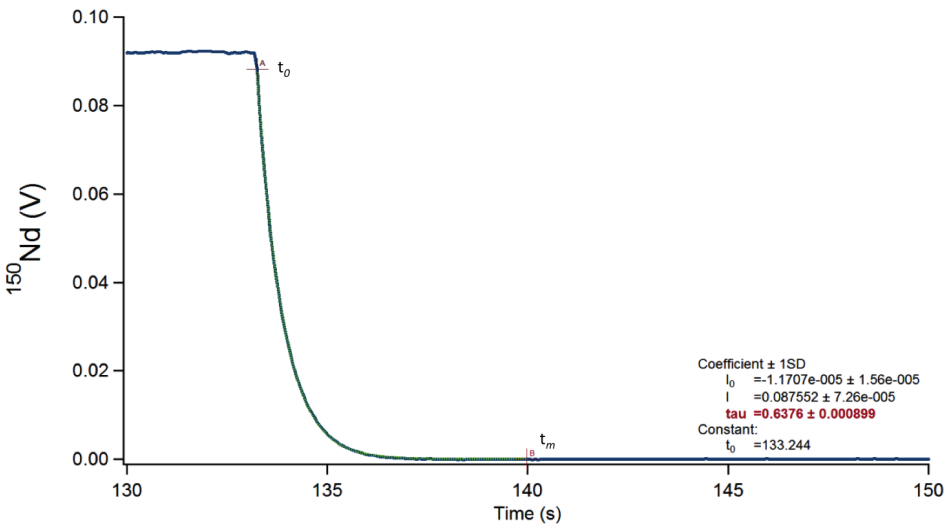

Figure 1. Fit of an exponential offset curve to the tau response curve of a 10^{13} Ω amplifier. Tau value (red) and uncertainty (1SD) are given in the legend.

Tau correction for 10^{13} Ω amplifiers

During tau rise and decay, the relationship between the measured integrated signal intensity (I_m) to the true signal intensity (I_t) can be described by an exponential offset equation.

(1) $$I_m = I_t + \Delta I e^{\left\{\frac{-t}{\tau}\right\}}$$

Where t is the duration time, τ is the tau constant and ΔI is the amplitude. Differentiating the exponential offset equation gives:

(2) $$\frac{dI}{dt} = \frac{-1}{\tau} \Delta I e^{\left\{\frac{-t}{\tau}\right\}}$$

Rearranging (1) and substituting into (2):

(3) $$\frac{dI}{dt} = \frac{-1}{\tau} \left(I_m - I_t\right)$$

Solving the equation for I_t yields:

(4) $$I_t = I_m + \frac{dI}{dt} \tau$$

The Neptune Plus MC-ICP-MS uses integrating detectors, where each output value is an average of the number of pulses measured during a set period of time. Consequently, the tau response curve described across a series of integrations is mirrored within each individual integration. (Figure 2). Therefore, equation (4) does not need not to be applied over the course of an entire decay, but on an integration-by-integration basis only. Using the method to calculate rate of change in Kimura *et al*[2], to correct isotope ratios collected with 10^{13} Ω amplifiers, then equation (4) can be rewritten as:

(5) $$I_t = I_m + \frac{I_{m+1} - I_{m-1}}{t_{m+1} - t_{m-1}} \times \tau$$

As the rate of change calculation requires the signal intensity of the prior and proceeding integrations, the first and last integrations of any run are lost. Equation (5) can be used with all integration times except 8 ms, where it fails to respond to the large and rapid deviations in signal. This observation is consistent with the tau correction approaches adopted by Pettke *et al.*[5]

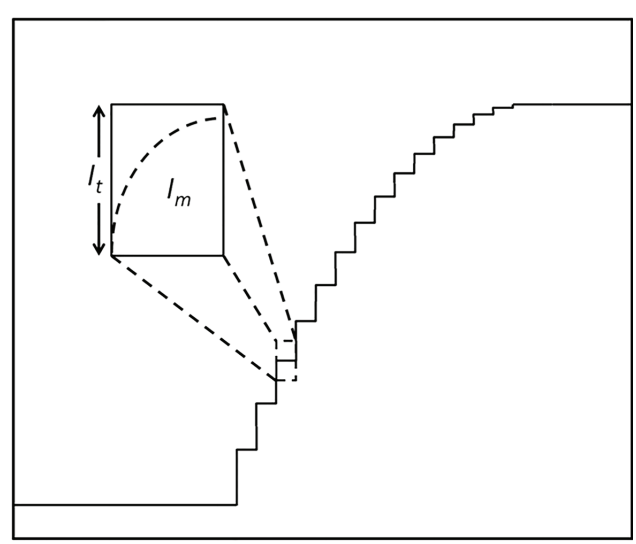

Figure 2. Representation of a tau response curve, across and within a series of integrations.

$^{208}Pb/^{206}Pb$ and $^{207}Pb/^{206}Pb$ isotope ratio analysis of four MPI-DING glasses by LA-MC-ICP-MS

10 spot ablations were performed on the four MPI-DING glasses, using the procedure previously outlined. An example of a spot ablation on GOR132-G is given in Figure 3. Without tau correction (Figure 3A) the rise in signal for ^{206}Pb lags significantly behind ^{208}Pb. The ^{206}Pb trace is also smoother, showing few of the transient changes in signal intensity exhibited on ^{208}Pb. Applying the tau correction (Figure 3B) transformed the shape of the ^{206}Pb signal trace to one that closely follows the ^{208}Pb trace.

Both ^{206}Pb and ^{208}Pb signals grew in and decayed at the same rate, and transient changes in signal are observed on both isotopes.

Even after cropping eight seconds from each spot ablation, the tau correction still had an appreciable impact on the isotope ratio precision (Figure 3C). For GOR132-G and StHs/680-G, using the tau correction, improved internal precision slightly, but the tau correction had a much more pronounced impact on the external precision of the 10 spot ablations and the relative difference (RD) to the reference values[10] (Table 3). For T1-G, the tau correction reduced the external RSD from 0.89‰ to 0.39‰, and the RD from 4.00‰ to -0.06‰. Without tau correction, the $^{208}Pb/^{206}Pb$ ratios for ATHO-G and T1-G were biased (outside uncertainty) towards ratios higher than the reference values. Following tau correction, the mean $^{208}Pb/^{206}Pb$ ratio for all four MPI-DING glasses was closer to the reference value.

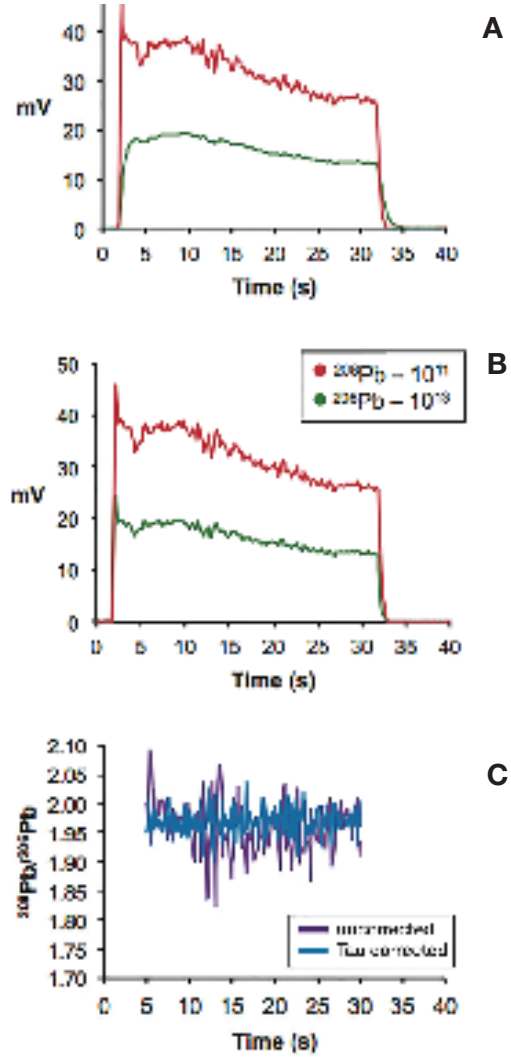

Figure 3. Spot ablation of GOR132-G, 40 µm spot size, 3 J cm^{-2} fluence, 8 Hz repetition rate, 30 s duration. ^{208}Pb – 10^{11} Ω amplifier, ^{206}Pb – 10^{13} Ω amplifier. (A.) ^{206}Pb not tau corrected. (B.) ^{206}Pb tau corrected. (C.) $^{208}Pb/^{206}Pb$, four seconds cropped from beginning and end.

Table 3. Pb isotope ratio results for four MPI-DING glasses. 40 µm spot size, 3 J cm^{-2} fluence, 8 Hz repetition rate, duration = 22 s, number of cycles = 164, n = 3. Tau correction was applied only to the $^{208}Pb/^{206}Pb$ isotope ratio. Relative Difference (RD) = mean value/reference value – 1. Reference values from 10.

		^{206}Pb	$^{208}Pb/^{206}Pb$			$^{207}Pb/^{206}Pb$	
			Both on 10^{11} Ω	^{206}Pb on 10^{13} Ω	^{206}Pb on 10^{13} Ω - Tau Corrected	Both on 10^{11} Ω	Both on 10^{13} Ω
ATHO-G	Mean	3.76 mV (235 kcps)	2.079	2.081	2.077	0.843	0.844
	Internal RSD (‰)		3.90	2.08	2.54	5.47	0.85
	External RSD (‰)		3.43	1.29	1.16	3.53	0.74
	RD (‰)		2.60	3.77	1.56	1.66	2.09
T1-G	Mean	6.62 mV (414 kcps)	2.081	2.089	2.081	0.838	0.838
	Internal RSD (‰)		2.32	1.84	1.88	3.43	0.49
	External RSD (‰)		1.05	0.89	0.39	1.40	0.83
	RD (‰)		-0.24	4.00	-0.06	0.63	0.10
StHs/680-G	Mean	7.84 mV (490 kcps)	2.039	2.042	2.040	0.826	0.827
	Internal RSD (‰)		1.94	2.14	1.68	2.78	0.45
	External RSD (‰)		1.63	1.57	0.68	1.48	0.62
	RD (‰)		0.68	2.22	0.90	-0.39	0.06
GOR132-G	Mean	16.2 mV (1 Mcps)	2.011	2.013	2.012	0.817	0.817
	Internal RSD (‰)		0.78	1.86	1.21	1.11	0.23
	External RSD (‰)		0.58	1.86	0.49	0.63	0.30
	RD (‰)		0.81	1.54	1.14	0.40	0.52

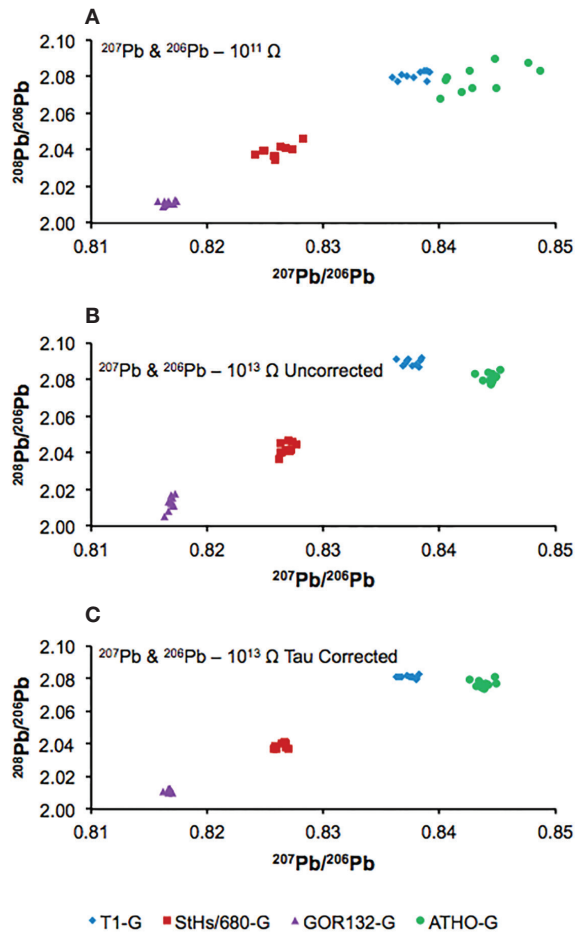

Figure 4. Determination of Pb isotope ratios of MPI-DING reference glasses by LA-MC-ICP-MS, using two amplifier configurations. (A) - ^{206}Pb, ^{207}Pb and ^{208}Pb all measured on 10^{11} Ω amplifiers. (B) ^{206}Pb and ^{207}Pb measured on 10^{13} Ω amplifiers. (C) ^{206}Pb and ^{207}Pb measured on 10^{13} Ω amplifiers, tau corrected.

Plots of ^{208}Pb/^{206}Pb against ^{207}Pb/^{206}Pb (Figure 4) highlighted the difference between measuring ^{207}Pb and ^{206}Pb on 10^{11} Ω amplifiers or 10^{13} Ω amplifiers, with or without tau correction. The ^{207}Pb/^{206}Pb ratio precision, both internal and external, was always improved using the 10^{13} Ω amplifiers. Prior to tau correction, measuring ^{206}Pb on a 10^{13} Ω amplifier only reduced the uncertainty on the ^{208}Pb/^{206}Pb ratio for ATHO-G and T1-G, the MPI-DING glasses with the lowest proportion of lead. Using tau correction the external precision on ^{208}Pb/^{206}Pb ratio, relative to the 10^{11} Ω amplifier, was improved on all four glasses.

StHs/680-G, average ^{206}Pb signal 7.84 mV, showed little change in ^{208}Pb/^{206}Pb precision between 10^{11} Ω (2.0393 ± 0.0033) and 10^{13} Ω amplifiers (2.0425 ± 0.0032). Tau correction of the 10^{13} Ω amplifier data, however reduced the uncertainty on the ^{208}Pb/^{206}Pb ratio (2.0398 ± 0.0014) by more than half (Figure 5).

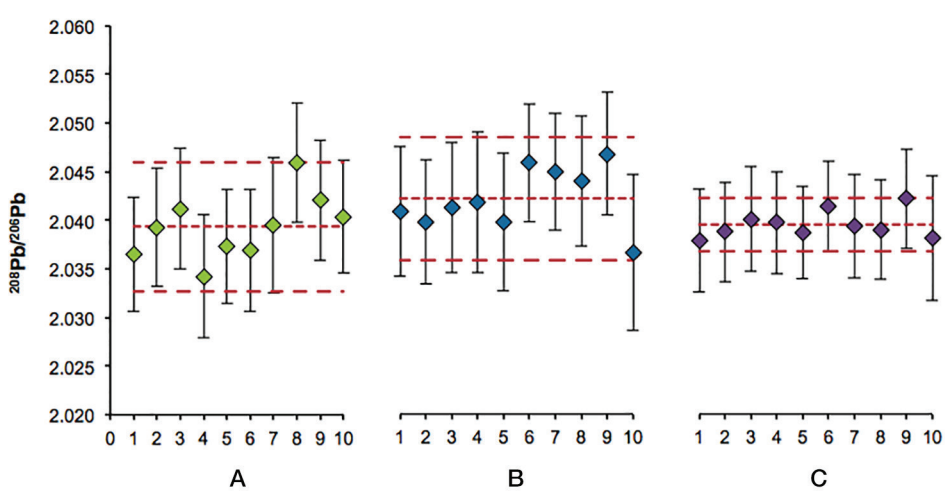

Figure 5. ^{208}Pb/^{206}Pb for 10 spot ablations of StHs/680-G. Error bars are 2SE. (A) ^{206}Pb, ^{207}Pb and ^{208}Pb all measured on 10^{11} Ω amplifiers. (B) ^{206}Pb and ^{207}Pb measured on 10^{13} Ω amplifiers. (C) ^{206}Pb and ^{207}Pb measured on 10^{13} Ω amplifiers, tau corrected. Red lines are mean values for all 10 runs and associated uncertainties (2SD).

Conclusion

Large variations in response time between different types of amplifiers reduces the effectiveness of high gain 10^{13} Ω amplifiers for many applications. Here we have demonstrated the utility of a dynamic tau correction to perform transient isotope ratio analysis by LA-MC-ICP-MS using 10^{13} Ω amplifiers. Once the tau constant has been determined for each amplifier, the correction can be applied over a series of runs, as it is not depended on factors such as integration time or signal intensity. Up to 4x improvement in precision were achieved for Pb isotope ratio analysis.

With this and related dynamic time corrections, the 10^{13} Ω amplifier technology can offer even greater benefits to multicollector mass spectrometry.

References

1. J. M. Koornneef, C. Bouman, J. B. Schwieters and G. R. Davies, *Anal. Chim. Acta*, **2014**, *819*, 49–55.
2. J.-I. Kimura, Q. Chang, N. Kanazawa, S. Sasaki and B. S. Vaglarov, *J. Anal. At. Spectrom.*, **2016**, 00, 1–11.
3. A. von Quadt, J.-F. Wotzlaw, Y. Buret, S. J. E. Large, I. Peytcheva and A. Trinquier, *J. Anal. At. Spectrom.*, **2016**.
4. M. Klaver, R. J. Smeets, J. M. Koornneef, G. R. Davies and P. Z. Vroon, *J. Anal. At. Spectrom.*, **2016**, *31*, 171–178.
5. T. Pettke, F. Oberli, A. Audétat, U. Wiechert, C. R. Harris and C. a. Heinrich, *J. Anal. At. Spectrom.*, **2011**, *26*, 475–492.
6. Z. Hu, Y. Liu, S. Gao, S. Xiao, L. Zhao, D. Günther, M. Li, W. Zhang and K. Zong, *Spectrochim. Acta Part B At. Spectrosc.*, **2012**, *78*, 50–57.
7. T. Hirata, Y. Hayano and T. Ohno, *J. Anal. At. Spectrom.*, **2003**, *18*, 1283.
8. T. Iizuka and T. Hirata, *Chem. Geol.*, **2005**, *220*, 121–137.
9. T. Iizuka, S. M. Eggins, M. T. McCulloch, L. P. J. Kinsley and G. E. Mortimer, *Chem. Geol.*, **2011**, *282*, 45–57.
10. K. P. Jochum, U. Nohl, K. Herwig, E. Lammel, B. Stoll and A. W. Hofmann, *Geostandards and Geoanalytical Research*, **2005**, *29*, 333-338

Find out more at **www.thermofisher.com/irms**

ThermoFisher SCIENTIFIC